Journal of Materials Science: Materials in Electronics (2019) 30:3482–3487
https://doi.org/10.1007/s10854-018-00624-y

Produce of carbon nanotube/ZnO nanowires hybrid photoelectrode for efficient dye-sensitized solar cells

Bayram Kilic[1]

Received: 12 November 2018 / Accepted: 21 December 2018 / Published online: 2 January 2019

Abstract
In this paper, we have successfully grown high quality CNT film on FTO substrate followed by ZnO NWs growth on top of CNT film by hydrothermal growth method. Dye-sensitized solar cells (DSSC) were fabricated utilizing carbon nanotube (CNT)/ZnO nanowire (NW) hybrid photoelectrode. By using the CNT/ZnO NWs in DSSC as photoanodes, it was shown that the hybrid structure is promising alternative in conventional DSSCs becuase CNT and ZnO show perfect work-function alignment, high surface area and superior optoelectronic properties. The fabricated DSSC shows a solar cell efficiency of $\eta = 5.55\%$, which is 20% higher than the cell fabricated without CNT layer. It was demonstrated that the incorporated CNT caused both enhancement of N719-dye absorption on the surface of hybrid structures and significant increase of short circuit current density (Jsc) due to longer electron lifetime. Current density (Jsc)-Voltage characterization indicates the enhancement of the power conversion efficiency of the solar cell mostly due to the increase of carrier density by CNT, decrease in carrier recombination and increase devices voltage. Based on the above results, we were able to obtain almost the highest power conversion efficiency among ZnO based DSSCs.

1 Introductıon

Nano-semiconductor materials have been studied great attention on their produce and characterization owing to the unique size and shape dependent properties and could be widely used in light emitting diodes, lasers, solar cells applications [1–3]. Recently, hybrid materials have been investigated as one of the most favorable candidates for thin film solar cell applications such as dye-sensitized solar cell (DSSC) [4]. DSSCs have been investigated conspicuously last decades due to low cost and non toxic device materials, and very easy fabrication [5]. Working principle of DSSCs is quite different from conventional p-n junction Si- based solar cells. In DSSCs, under solar irradiation, dye molecules are excited from highest occupied molecular orbital level (HOMO) to lowest unoccupied molecular level (LUMO). Excited electrons are injected conduction band of semiconductors based photoanode such as TiO_2 or ZnO. This process is called electron injection process. The injected electron is moved through the photoanode to the FTO or ITO back contact of the working electrode (WE). Meanwhile, depleted dye take an electron from I^-/I^-_3 redox couple flew from an external circuit. The circuit is connected to the Pt counter electrode (CE) and Pt CE give an electron to redox couple. As a result, photo converted electron flows through the external devices [6]. The most important parameters in DSSCs in respect to high solar efficiency are the photoanode. We used CNT/ZnO NWs as photoanode in DSSCs. ZnO has been attracted much attention within the scientific community as a 'new generation material' for electronic, optic and solar cell applications. ZnO has a wide and direct band gap energy ~ 3.37 eV, suitable for DSSC applications due to higher electronic mobility that would be favorable for electron transport, with reduced recombination loss and high exciton-binding energy ~ 60 meV, which is make promising candidate for room temperature optoelectronic devices [7, 8] [7, 8]. ZnO is also grown very easily as nanostructures with different surface morphologies such as nanowire, nanorods, nanotube [9]. Among different ZnO nanostructures, ZnO NWs have been studied because one dimensional ZnO NWs show quantum confinement effects and high surface area [10]. ZnO NWs are used as ideal materials for studying the transport process in one-dimensional confined materials, which are useful for understanding the fundamental principle of low dimensional devices and investigating new

✉ Bayram Kilic
bkilic@yalova.edu.tr

[1] Department of Energy Systems Engineering, Faculty of Engineering, Yalova University, 77100 Yalova, Turkey

concept solar cells such as DSSCs with high performance [11]. Although 1D-ZnO NWs have been widely used in DSSCs, compared with the others cells such as TiO_2 based DSSCs or silicon solar cells, power conversion efficiency was still low and unsatisfied [12]. CNT could offer a potential platform to enhancement surface area and decrease of carrier recombination in DSSCs [13]. CNTs have an extraordinary electro-optic and mechanical properties making them promising candidate for improving the charge transport and short circuit current [14]. In this study, we produce CNT/ZnO NWs based hybrid solar cells and explain their electrical, optical and chemical properties using various characterization methods. The effect of CNT/ZnO NWs photoanode on power conversion efficiency of DSSCs was investigated with comparison to pure ZnO NWs based cell and it was shown that power conversion efficiency was increased from 5.05% to 5.55% corresponding to 9.9% enhancement.

2 Experimental

2.1 Preparation of A-CNT/ZnO hybrid photoanodes

Produce of CNTs were carried out by CVD (Chemical Vapor Deposition) on silicon substrate by using an iron/aluminum oxide catalyst (1/10 nm) deposited by electron beam evaporation. Details of deposition mechanism are described in our previous work [6]. Briefly, the produce of CNT was carried out at 850 °C, rewarding an average deposition rate, which is including nucleation and growth, of ~2 μms^{-1}. Vertically aligned CNTs were synthesized on silicon wafers (1 cm^2) with densities of 10^9-10^{10} CNTs cm^{-2}. After then, vertically-aligned CNTs were dispersed onto a FTO (F:SnO_2) substrate via contact printing method. After the growth of CNT, ZnO NWs were grown on FTO/CNT substrate by hydrothermal method. 0.1 g zinc nitrate hexahydrate and 25 ml D^+H_2O were prepared in a magnetic stirrer and 6 mL NH_3 in of portion 28% was put into the solution. The solution was moved into an autoclave. The FTO/CNT substrates were plunged into the solution, and the autoclave was heated to 175 °C for 12 h. After the growth, the obtained ZnO nanowires coated on CNT/FTO substrate and CNT/ZnO NW were annealed in a furnace at 300 °C in air for 30 min to obtain the DSSC photoanodes.

2.2 Device fabrication of DSSCs based on A-CNT/ZnO Hybrid photoanodes

CNT/ZnO photoanode was prepared by absorption of N719 dye molecules for 12 h. The CNT/ZnO was heated to 90 °C for 60 min before immersing into a 0.5 mM solution of the N719 dye. CNT/ZnO photoanode were taken out, rinsed with acetonitrile, and dried with nitrogen gas. The dye-sensitized CNT/ZnO photoanode with Pt counter electrode were sandwiched together using a 20 μm thick transparent Surlyn film (Meltonix 1170, Solaronix). The electrolyte, which consists of 0.5 M tetrabutylammonium iodide, 0.05 M I_2 and 0.5 M 4-tertbutylpyridine in acetonitrile, was injected between two electrodes and well distributed via capillary action. The active electrode area was typically 0.25 cm^2 for all type of cells studied in this work.

2.3 Characterization of the device

The surface morphology of the CNT/ZnO nanostructures was examined using Philips XL30 ESEM-FEG scanning electron microscope equipped with an EDAX (or EDS) energy dispersive X-ray spectroscopy detector. Crystal structure analysis was carried out using X-ray diffraction (XRD; Rigaku D/Max-IIIC diffractometer) with 1.54 Å Cu-Kα radiation and 2θ range of 20–80°. The topographic and surface images of films were investigated simultaneously by contact mode atomic force microscope (AFM, JPK, NanoWizard). The Raman scattering measurements were performed using a micro Raman Renishhaw 2000 system with an excitation source of 514.5 nm at RT. The infrared spectra were recorded using Fourier-transform infrared (FTIR) spectrometer, Perkin Elmer, in transmittance mode at 450–4000 cm^{-1}. Photocurrent density versus voltage (J-V) data were recorded using a Keithley 175A digital multimeter using a 0.01 V/s voltage ramp rate and an AM 1.5 solar simulator.

3 Results and discussion

Surface investigation of CNT/ZnO NWs hybrid structures were carried out using AFM and SEM images. Schematic illustration of CNTs on FTO substrate was shown in Fig. 1a. As seen in schematic illustration, CNT nanostructures were tried to obtain with certain spacing. Figure 1b shows that the CNT were produced on the substrate with 30–50 nm spacing and it is demonstrated that pure CNT nanostructures were homogenously coated on an FTO substrate. Carbon nanotubes have greatly applications, where properties of their nanostructures could depend on interspacing distances. Interlayer spacing of CNTs is not a constant and ranges from 1 nm to 100 nm. Mechanical and electrical properties of CNTs are closely related to those distances. Although CNTs would bring many benefits to the transport of electrons, improvement in photovoltaic performance of the DSSCs can be explained at a very narrow spacing of CNTs in the photoanode. When the interlayer spacing of CNTs exceeds the optimized value, the short circuit current and photovoltaic power efficiency of the cells decrease rapidly. However, it is of great importance to arrange of optimized value of CNT

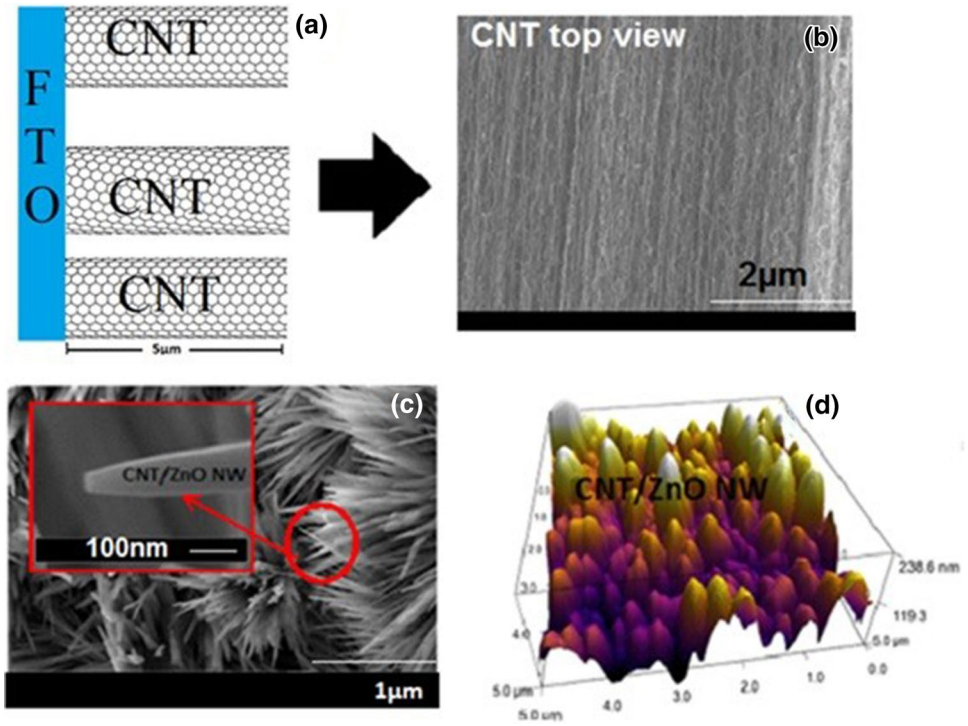

Fig. 1 **a** Schematic illustration of CNT, **b** SEM images of CNT grown on FTO, **c** CNT/ZnO NW with different magnification; **d** topography images of the CNT/ZnO NW obtained using AFM contacting mode

spacing could give extraordinary electronic and mechanical results. In this study, CNT can be growth on substrate with 1% volume fraction as dependent on experimental procedure. This value of CNT gives about 20–50 nm interlayer spacing and lead high absorption of N719 dye molecules, which harvests more photon and leads to more electrons injected from N719 dye into CB of ZnO. On the other hand, ZnO NWs can be grown on CNTs with extremely high aspect ratio. SEM images taken on a hydrothermally grown ZnO NWs on CNT are demonstrated in Fig. 1c. The ZnO NWs were grown vertically on CNT with an average diameter of 40 nm and length up to about five micrometers. In addition to SEM images, AFM measurements were carried out to investigate surface morphology of CNT/ZnO NWs as seen in Fig. 1d. AFM measurements show that the Zn NWs have vertical aligned 1-D crystal structures. These images also indicated that the ZnO nanowires have an about 10–15 nm diameter and 100 nm in length. Surface image results demonstrated that AFM measurements give extraordinary topographic constant direct height measurements, and three-dimensional surface image of the ZnO NWs.

Chemical characterization of the CNT/ZnO NWs is examined by Energy-dispersive X-ray spectroscopy (EDS). The EDS measurements of CNT/ZnO NW hybrid system is shown in Fig. 2a. The EDS measurements demonstrate the presence of Zn, O, C and Si. Si peak come to FTO glass substrate. Results indicated that we can grow CNT based ZnO NWs hybrid structures with homogenous distribution.

Figure 2b demonstrates the FTIR spectrum of CNT/ZnO NW recorded in the range of $4000-500\ cm^{-1}$. The band located near $595\ cm^{-1}$ can be attributed to the Zn-O stretching mode. FTIR peak at $795\ cm^{-1}$ corresponds to CNT bond in the ZnO. The band at $3200\ cm^{-1}$ to $3600\ cm^{-1}$ related to the stretching vibration of -OH groups. The synthesized CNT/ZnO NWs were investigated by XRD characterization to explain the crystal structures of the CNT/ZnO NWs. The diffraction peaks at 25° belongs to the (002) crystal structures of CNT and the ZnO NWs possess the wurtzite hexagonal structure with high crystallinity as seen in Fig. 2d. Strong (100), (002), and (101) peaks showed that the sample consists of well-aligned ZnO NWs on CNT. Raman measurements were carried out to investigate the vibration properties of the CNT/ZnO NW thin films (Fig. 2d). We indicated that a strong intensity Raman peak at $438\ cm^{-1}$ shows the spectrum known as the optical phonon E_2 in ZnO nanostructures and this mode related to the band characteristic for the wurtzite ZnO structures. On the other hand, two Raman peaks at 331 and $380\ cm^{-1}$ were known to be as E_{2H}-E_{2L} (multi phonon) and A_{1T} modes, respectively. Raman peak at $582\ cm^{-1}$ known to be related to the E_1 mode due to the oxygen deficiency[18] indicates the presence of oxygen vacancies in the ZnO NWs. Raman peaks at around 1310 and $1590\ cm^{-1}$ are related to the characteristic D-band and G-band of carbon groups such as carbon nanotube. XPS spectra of CNT/ZnO NW samples are shown in Fig. 3a-d. It may be seen that the $Zn2p_{3/2}$ and Zn $2p_{1/2}$ can be fitted into

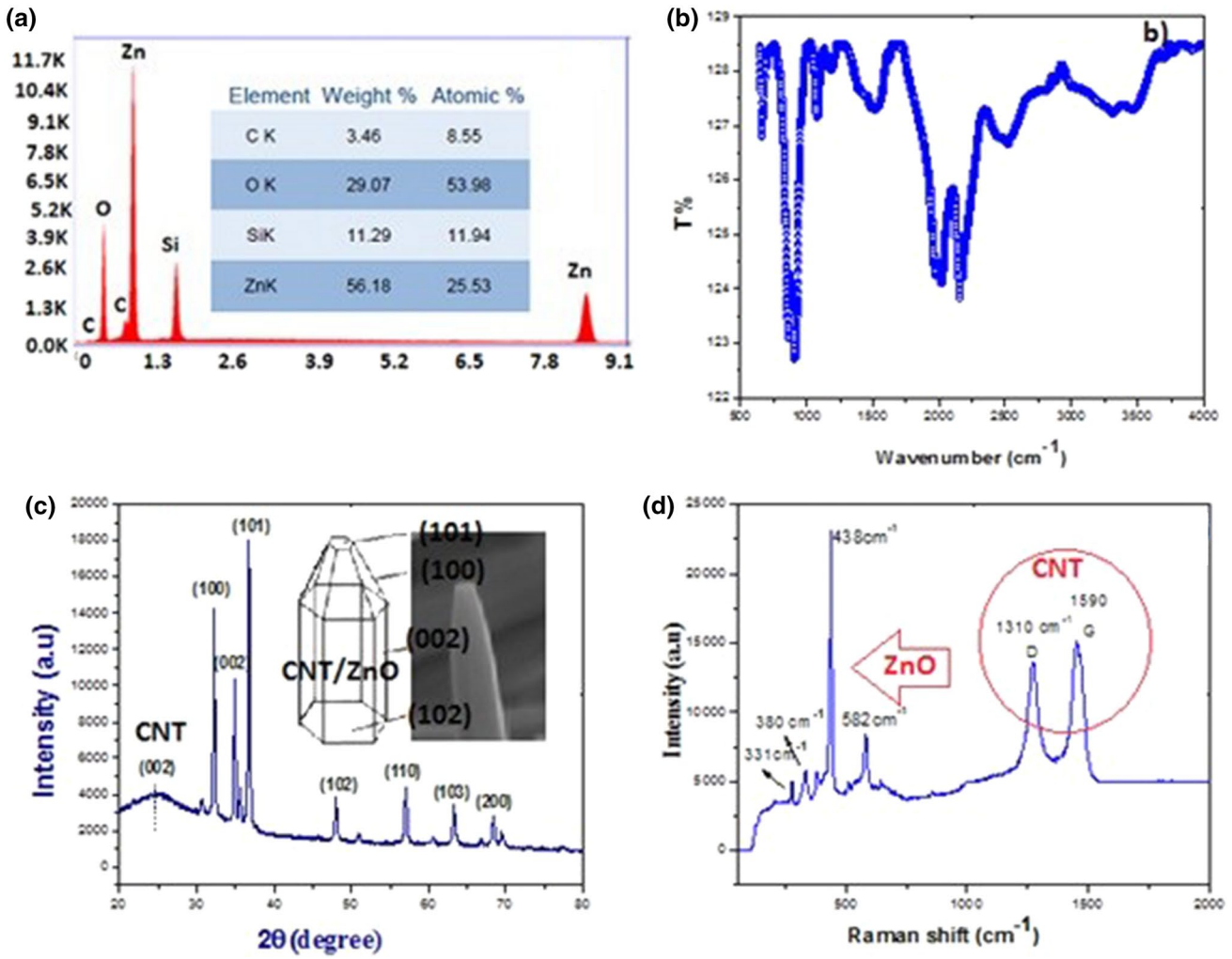

Fig. 2 **a** EDS spectrum of the CNT/ZnO NW; **b** FTIR analysis of the CNT/ZnO NW; **c** Crystal structure analysis was carried out using X-ray diffraction (XRD; Rigaku D/Max-IIIC diffractometer) with 1.54 Å Cu-Kα radiation and 2θ range of 20–80° of the the CNT/ZnO NW; **d** Raman spectra of the the CNT/ZnO NW with the Ar^+ (514.5 nm) laser line as the exciton sources

1020 and 1043 eV, respectively. O 1 s spectrum can be fitted into peaks 530.0 eV and it is attributed to Zn-O bonding. XPS spectrum shows three 268.0, 283.5 and 291.0 eV peaks corresponding to C 1 s spectrum. The C 1 s peak at 286.4 eV and strong O 1 s peak at 530.0 eV are known to be owing to the O-C-O complex.

Device structure and photovoltaic characterization of the CNT/ZnO NWs are illustrated in Fig. 4a, b. As seen in Fig. 4a, CNT/ZnO NW based DSSC architecture can be used as a new alternative to the conventional DSSC structures. We used the photocurrent density–voltage (J-V) characterization to investigate the photovoltaic energy conversion efficiency (PEC) of CNT/ZnO NW DSSC. Figure 4b shows the J-V measurements of two electrodes with CNT and without CNT. While DSSC with CNT electrode shows Jsc and PEC efficiency as 16.13 mA/cm^2 and $\eta = 5.55\%$, respectively, DSSC without CNT electrode shows 14.47 mA/cm^2 and $\eta = 5.05\%$, respectively (Table 1). In the presence of 1% wt volume fraction CNT, Jsc increases by ~ 20%. The use of CNT gives high absorption of N719 dye molecules, which harvests more photon and leads to more electrons injected from N719 dye into CB of ZnO. When ZnO NWs were homogeneously grown on CNT substrate, we can obtain the effective and continuous conductive network. The short circuit current density of the CNT/ZnO NW junctions is larger than that obtained from the pure ZnO NW. Due to the high Jsc of the CNT/ZnO NW cell, its PEC efficiency was increased as compared to the pure ZnO cell. The increased Jsc of CNT/ZnO NWs is mainly contributed to the increased of surface area in the hybrid structures. Electrons in the network get very long mean free paths, escape charge recombination, and extend the electron lifetime. We show that the electrons transportation from conduction band of ZnO

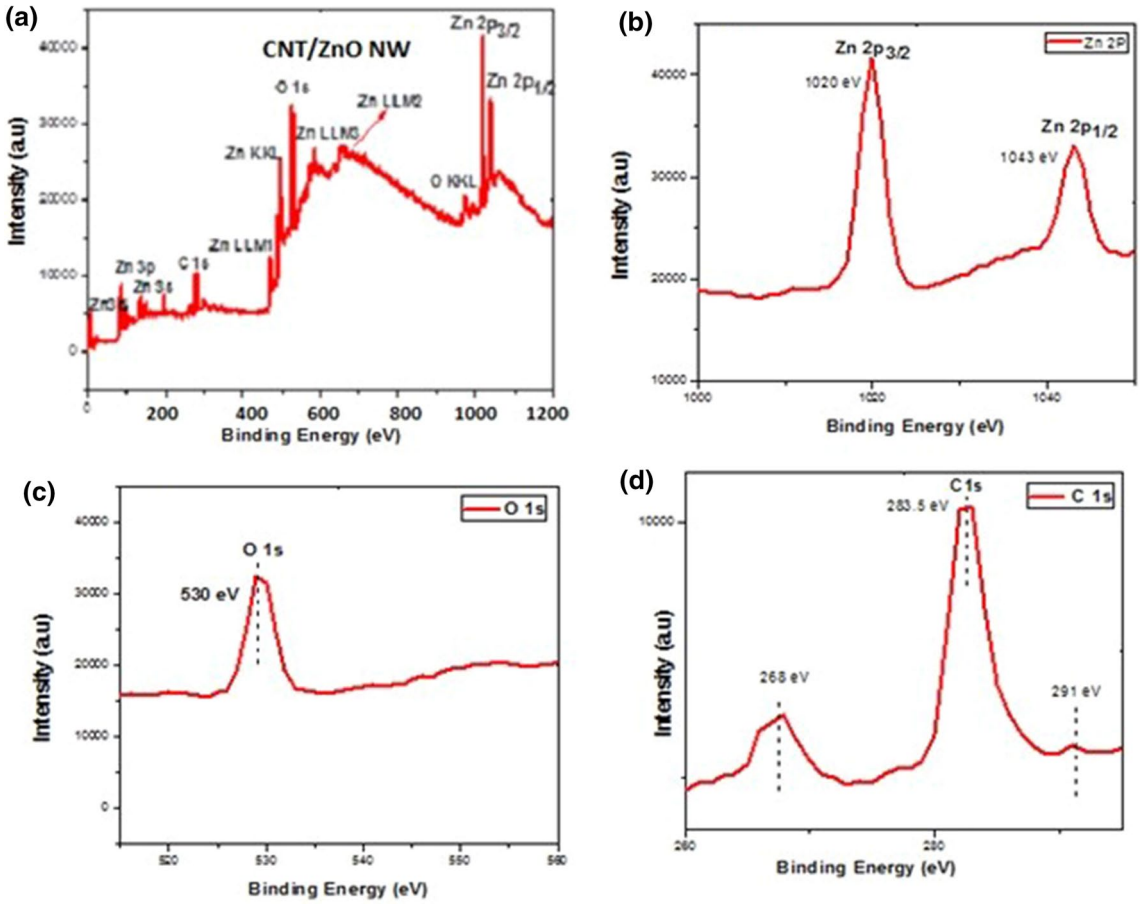

Fig. 3 XPS spectra of CNT/ZnO NW **a** Wide scan XPS, **b** Zn_{2p}, **c** O_{1S}, **d** C_{1S}

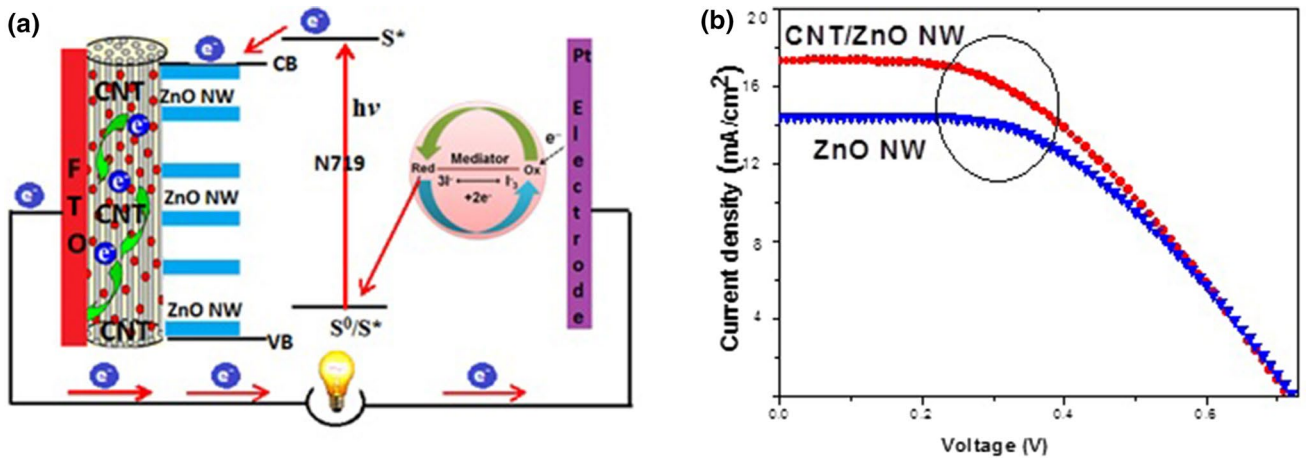

Fig. 4 **a** Design and band-gap engineering of CNT/ZnO NW, **b** J-V characterization of CNT/ZnO NW

Table 1 Photovoltaic properties of CNT/ZnO NW and pure ZnO NW structures, measurements were performed under AM 1.5G one sun (light intensity: 100 mW cm^{-2})

Sample	FF (%)	η (%) (efficiency)	Voc (V)	Jsc (mA/cm^2)
ZnO NW	49	5.05	0.71	14.47
CNT/ZnO NW	45	5.55	0.71	16.13

The active area was set at 0.25 cm^2 for all of the cells

NWs to CNTs is carried out very quickly, just as shown in Fig. 4a. Under incident light irradiation, electrons from dye molecules are excited to upper level and excited electrons are injected into conduction band of ZnO NWs. The injected electron is moved onto CNTs. CNTs show a significant improvement in performance of CNT/ZnO NW based DSSCs due to increase of dye adsorption rate and long electron lifetime.

4 Conclusions

We introduce that the properties of CNT/ZnO NW depend on the surface morphology, and the role of optimum experimental parameters improve the dye molecules loading and minimize the charge recombination. CNT/ZnO NW are synthesized on FTO ($F:SnO_2$) substrate using an easy and very chip growth technique. As different literature, in this study first time, we can growth vertically aligned ZnO NW on carbon nanotube without disturbing of tube spacing by hydrothermal method. In this work, we explain the role of CNTs in the semiconductor electrodes by investigating and comparing the electronic process in the dye-sensitized photovoltaic devices. Until now, the highest solar conversion efficiency of CNT/ZnO nanostructures has been obtained around 6,20%. In this study, we show that the CNT/ZnO NW show enhanced Jsc and efficiency as compared with pure ZnO cells. CNT/ZnO NW solar cell is 5.55%, which is higher than that of pure ZnO cell (5.05%). The improvement in the photovoltaic efficiency is owing to the fact that CNT reduce the electrolyte/electrode interfacial resistance, the recombination and enhances the transport of electrons from the photoanode to FTO substrate, respectively. Further, the increase in dye adsorption rate is due to the increased surface area (CNT in ZnO) and improved inter connectivity between the ZnO and CNT are also the particular reasons for the enhancement in the Jsc and efficiency.

References

1. M. Salavati-Niasari, S.M. Hosseinpour-Mashkani, F. Mohandes, S. Gholamrezaei, Synthesis, characterization and photovoltaic studies of $CuInS_2$ nanostructures. J. Mater. Sci.: Mater. Electron. **May 1;26**(5), 2810–2819 (2015)
2. S.M. Hosseinpour-Mashkani, A. Sadeghinia, Z. Zarghami, K. Motevalli, $AgInS_2$ nanostructures: sonochemical synthesis, characterization, and its solar cell application. Journal of Materials Science: Materials in Electronics. 2016 Jan 1;27(1):365–74
3. H. Zeynali, S. Alvarzandi, S.M. Hosseinpour-Mashkani, In_2S_3 nanostructures: semi-batch synthesis and characterization and its photovoltaic applications. J. Mater. Sci.: Mater. Electron. **Jun 1;26**(6), 4265–4272 (2015)
4. M. Grätzel, Dye-sensitized solar cells. J. Photochem. Photobiol., C **31**(2), 145–153 (2003 Oct) 4(
5. A. Hagfeldt, G. Boschloo, L. Sun, L. Kloo, H. Pettersson, Dye-sensitized solar cells. *Chemical reviews*. 2010 Sep 10;110(11):6595–663
6. B. Kilic, S. Turkdogan, A. Astam, O.C. Ozer, M. Asgin, H. Cebeci, D. Urk, S.P. Mucur, Preparation of carbon nanotube/TiO_2 mesoporous hybrid photoanode with iron pyrite (FeS_2) thin films counter electrodes for dye-sensitized solar cell. Scientific reports **31**, 6:27052 (2016 May)
7. Q. Wan, Q.H. Li, Y.J. Chen, T.H. Wang, X.L. He, J.P. Li, C.L. Lin, Fabrication and ethanol sensing characteristics of ZnO nanowire gas sensors. Appl. Phys. Lett. **3**(18), 3654–3656 (2004 May) 84(
8. M. Mansournia, S. Rafizadeh, S.M. Hosseinpour-Mashkani, An ammonia vapor-based approach to ZnO nanostructures and their study as photocatalyst material. Ceramics International. 2016 Jan 1;42(1):907–16
9. B. Kilic, S. Turkdogan, Fabrication of dye-sensitized solar cells using graphene sandwiched 3D-ZnO nanostructures based photoanode and Pt-free pyrite counter electrode. Mater. Lett. **15**, 193:195–198 (2017 Apr)
10. P. Raksa, S. Nilphai, A. Gardchareon, S. Choopun, Copper oxide thin film and nanowire as a barrier in ZnO dye-sensitized solar cells. Thin Solid Films **Jul 1;517**(17), 4741–4744 (2009)
11. C.H. Lee, W.H. Chiu, K.M. Lee, W.H. Yen, H.F. Lin, W.F. Hsieh, J.M. Wu, The influence of tetrapod-like ZnO morphology and electrolytes on energy conversion efficiency of dye-sensitized solar cells. Electrochim. Acta **Dec 1;55**(28), 8422–8429 (2010)
12. G.J. Chang, S.Y. Lin, J.J. Wu, Room-temperature chemical integration of ZnO nanoarchitectures on plastic substrates for flexible dye-sensitized solar cells. Nanoscale. **6**(3), 1329–1334 (2014)
13. W.C. Chang, Y.Y. Cheng, W.C. Yu, Y.C. Yao, C.H. Lee, H.H. Ko, Enhancing performance of ZnO dye-sensitized solar cells by incorporation of multiwalled carbon nanotubes. Nanoscale research letters **Dec 1;7**(1), 166 (2012)
14. A. Omar, H. Abdullah, M.A. Yarmo, S. Shaari, M.R. Taha, Morphological and electron transport studies in ZnO dye-sensitized solar cells incorporating multi-and single-walled carbon nanotubes. J. Phys. D: Appl. Phys. **27**(16), 165503 (2013 Mar) 46(